Published in final edited form as:
Magn Reson Med. 2012 January ; 67(1): 42–49. doi:10.1002/mrm.22970.

Calibration and validation of TRUST MRI for the estimation of cerebral blood oxygenation

Hanzhang Lu[1,*], **Feng Xu**[1], **Ksenija Grgac**[2,3,4], **Peiying Liu**[1], **Qin Qin**[2,4], and **Peter van Zijl**[2,4]

[1]Advanced Imaging Research Center, University of Texas Southwestern Medical Center, Dallas, Texas, United States

[2]F.M. Kirby Center for Functional Brain Imaging, Kennedy Krieger Institute, Baltimore, Maryland, United States

[3]Department of Chemistry, The Johns Hopkins University, Baltimore, Maryland, United States

[4]Department of Radiology, The Johns Hopkins University, Baltimore, Maryland, United States

Abstract

Recently, a T2-Relaxation-Under-Spin-Tagging (TRUST) MRI technique was developed to quantitatively estimate blood oxygen saturation fraction (Y) via the measurement of pure blood T2. This technique has shown promise for normalization of fMRI signals, for the assessment of oxygen metabolism, and in studies of cognitive aging and multiple sclerosis. However, a human validation study has not been conducted. In addition, the calibration curve used to convert blood T2 to Y has not accounted for the effects of hematocrit (Hct). In the present study, we first conducted experiments on blood samples under physiologic conditions, and the Carr-Purcell-Meiboom-Gill (CPMG) T2 was determined for a range of Y and Hct values. The data were fitted to a two-compartment exchange model to allow the characterization of a three-dimensional plot that can serve to calibrate the in vivo data. Next, in a validation study in humans, we showed that arterial Y estimated using TRUST MRI was 0.837±0.036 (N=7) during the inhalation of 14% O2, which was in excellent agreement with the gold-standard Y values of 0.840±0.036 based on Pulse-Oximetry. These data suggest that the availability of this calibration plot should enhance the applicability of TRUST MRI for non-invasive assessment of cerebral blood oxygenation.

Keywords

T2 relaxation under spin tagging; arterial spin labeling; cerebral blood flow; hypoxia; normoxia

Introduction

The brain's blood oxygenation (Y) and its arteriovenous difference ($Y_a - Y_v$) provide important information about the balance between oxygen demand and supply, and can be used to estimate other physiological parameters including oxygen extraction fraction (OEF) and cerebral metabolic rate of oxygen (CMRO2) (1–4). The oxygenation differences between resting and activated states also play a key role in the quantitative interpretation of the BOLD fMRI signal (5–8). Recently, a T2-Relaxation-Under-Spin-Tagging (TRUST) MRI technique was developed to quantitatively estimate Y via the measurement of pure blood T2 (9). Compared to other methods (10–16), this approach uses the spin labeling

[*]Corresponding Author: Hanzhang Lu, Ph.D. Advanced Imaging Research Center UT Southwestern Medical Center 5323 Harry Hines Blvd. Dallas, TX 75390 hanzhang.lu@utsouthwestern.edu Tel: 214-645-2761 Fax: 214-645-2744.

principle to isolate blood signal from surrounding tissue (17,18), thereby avoiding manual selection of regions-of-interest (ROIs) or the requirement that imaging voxel size be smaller than the vessel lumen. Using spatially non-selective T2 preparation pulses, this approach also minimizes the influence of flow velocity on T2 estimation. This technique has shown promise for normalization of fMRI signals (19,20) and for the measurement of CMRO2 (3), and has also been used in studies of cognitive aging (21) and multiple sclerosis (22). Methodological studies have also confirmed the sensitivity of this technique to physiologic procedures. TRUST-derived Y_v values increased with hypercapnia and hyperoxia (23,24), but decreased with caffeine uptake (9). However, a human in situ validation study of absolute oxygenation values has not yet been conducted for TRUST MRI.

To properly validate this technique, potential confounding factors in the Y estimation should be accounted for. One data processing step of the TRUST method involves the conversion of the experimentally determined T2 to blood oxygenation using a calibration plot, which specifies the relationship between these two parameters. To date, most studies using TRUST or other similar methods have assumed that blood T2 is primarily dependent on oxygenation (9,11,13,25), but in fact anther variable, hematocrit (Hct), also has a significant influence on T2 (26–29). Thus, the conversion from T2 to oxygenation should be conducted in the context of Hct, which could differ slightly across individuals.

In the present study, we first used experiments in blood samples to determine a three-dimensional (3D) calibration plot of blood T2 as a function of both Y and Hct. Next, we used a human hypoxia challenge to control blood oxygenation and compared TRUST-derived arterial Y values to those measured with the gold-standard Pulse Oximeter (PulsOx). In using this procedure, we took advantage of the fact that, unlike venous oxygenation, the brain's arterial oxygenation is identical to that in periphery and can be conveniently measured with non-invasive techniques such as PulsOx.

Methods

Calibration study

Experiments on blood samples were performed on a 3 Tesla MRI system (Achieva, Philips Medical Systems, The Netherlands) using a quadrature head coil for radiofrequency (RF) transmission and reception. Sample preparation was similar to that used in our previous studies (27,30). Briefly, bovine blood, which has physiologic and MR properties comparable to human blood (31), was circulated in a tube to avoid precipitation. The temperature was controlled to be 37°C using a water bath and was monitored with a fiber optic sensor (Oxford Optronix, Oxford, UK). Oxygenation was controlled with a gas chamber and determined with a blood analyzer (Radiometer America Inc., Westlake, OH). Five Hct levels (controlled through mixing of plasma and blood cells) within the physiologic range (0.35–0.55) were studied. At each Hct level, four physiologically relevant oxygenation levels (0.4–1) were investigated.

Once the sample condition reached a stable state, the TRUST sequence was performed. For the case of blood samples, there is no partial voluming between blood and tissue or the need for control/label subtraction, thus only control images were acquired. Under each sample condition, four TRUST scans were performed with inter-echo spacing (τ_{CPMG}) of 5, 10, 15 and 20 ms, respectively. For each TRUST scan, images with four different levels of T2-weighting were acquired and these were achieved by placing 0, 4, 8 or 16 non-slice-selective preparation pulses before the excitation pulse. Specifically, TRUST scan with τ_{CPMG} of 5ms used T2-preparation duration of 0, 20, 40, and 80 ms. TRUST with τ_{CPMG} of 10ms used T2-preparation duration of 0, 40, 80, and 160 ms. TRUST with τ_{CPMG} of 15ms used T2-preparation duration of 0, 60, 120, and 240 ms. TRUST with τ_{CPMG} of 20ms used T2-

preparation duration of 0, 80, 160, and 320 ms. Identical number of T2-preparation pulses was used for scans with different τ_{CPMG} so that the influence of RF pulse imperfection is comparable. Even though the human experiment in the present study only used a τ_{CPMG} of 10 ms, the establishment of blood T2 as a function of Y and Hct at other inter-echo spacings may be useful for future studies, thus these results are also included in this report. Other imaging parameters were: field-of-view (FOV) 64×64 mm^2, matrix 32×32, slice thickness 5 mm, single-shot gradient-echo EPI, TR/TE/flip angle=8000ms/8ms/90°, half scan factor = 0.89, composite ($90°_x 180°_y 90°_x$) block pulses for T2-preparation, MLEV16 RF phase cycling for multiple pulses, scan duration 2 minutes (9).

Mono-exponential fitting of the MR signal as a function of the T2-preparation duration, termed effective TE, yielded the blood T2 value. To establish an analytical relationship between T2, Y and Hct, we used a two-compartment exchange model described by Wright et al. (10) and Golay et al. (13). By combining Equations [3–6] in Golay et al. (13) (see Appendix for derivations), we obtained the following relationship:

$$\frac{1}{T_2}=A+B\cdot(1-Y)+C\cdot(1-Y)^2 \quad [1]$$

in which the coefficients A, B and C are in turn dependent on Hct by:

$$A=a_1+a_2\cdot Hct+a_3\cdot Hct^2 \quad [2]$$

$$B=b_1\cdot Hct+b_2\cdot Hct^2 \quad [3]$$

$$C=c_1\cdot Hct\cdot(1-Hct) \quad [4]$$

. The experimental data at different Hct and Y values were fitted to the model using a Matlab (Mathworks, Natick, MA) function, nlinfit, yielding six coefficients, a_1, a_2, a_3, b_1, b_2, and c_1. Note that, after characterization of the relationship between T2, Y and Hct, the knowledge of two parameters should allow the estimation of the third, which was used in the validation study.

Validation study

The human experiments were performed on a 3T using body coil for RF transmission and an eight-channel sensitivity encoding (SENSE) head coil for receiving. Foam padding was used to stabilize the head and minimize motion. The protocol was approved by University of Texas Southwestern Medical Center's Institutional Review Board and informed written consent was obtained from each participant. Seven healthy subjects (3 men and 4 women, 28.9 ± 4.0 years of age) participated in this study.

Before the subject entered the bore of the magnet, a nose clip and a mouth piece were attached so that he/she could breathe through the mouth only. The mouth piece was attached to a two-way non-rebreathing valve (Hans Rudolph, 2600 series, Shawnee, KS) through which the researcher can control the type of inspired air (32). During the experiment, the subject first breathed room-air for eight minutes while survey, SENSE reference scan, and a (normoxia) TRUST scan were performed. Then the breathing air was switched to 500L bag

containing 14% O2 and 86% N2 (equivalent to an altitude of 3,600 meters). From test data acquired outside MRI, we determined that it takes approximately 10 minutes after the gas switching for the physiologic parameters (e.g. O2 and CO2 levels) to reach a new steady state. Thus, a waiting period of 10 min was used to allow the arterial oxygenation to stabilize before a second (hypoxia) TRUST was performed. The following physiologic parameters were monitored and recorded throughout the MRI session: arterial oxygen saturation fraction (Y_a, in fraction) and heart rate (in beats per minute, bpm) were measured with a PulsOx device attached to a finger (MEDRAD, Pittsburgh, PA), End-tidal (Et) CO2 (in mmHg) and breathing rate (in breaths per minute, bpm) were measured with a capnograph device (Capnogard, Model 1265, Novametrix Medical Systems, CT). After the MRI scans were completed and the subject exited the scanner room, a blood sampling with a potassium ethylenediaminetetraacetic acid (EDTA) coated 10ml lavender tube was conducted on the basilic vein of the arm and Hct was measured with a centrifuge (Hemata STAT II, Separation Technology, Inc., Altamonte Springs, FL).

TRUST MRI measured T2 of the blood in cerebral arteries. A balanced pseudo-continuous labeling scheme (33,34) was used with a labeling duration of 800ms and a short delay of 200ms. Based on arterial transit times measured previously for labeling and imaging locations comparable to this study (~1 sec) (35,36), the use of these imaging parameters is expected to highlight arterial blood in large arteries before they entered intracortical arteries or arterioles. Major arteries are preferred over smaller arteries, which are known to have a lower Hct (37), because our blood sampling and Hct measurement were conducted in the large vessels. The blood labeling position was chosen to be 84 mm below the anterior-commissure (AC) posterior-commissure (PC) line, based on a previous study (38). The imaging slice consisted of a single axial slice positioned at 10 mm above the AC-PC line. The other components of the TRUST sequence were similar to those used previously (9). The imaging parameters were: FOV 240×240 mm^2, matrix 64×64, voxel size 3.75×3.75×10 mm^3, TR=2522 ms, four T2-weightings with the following effective TEs (associated with T2-preparation): 0ms, 40ms, 80ms and 160ms, with a τ_{CPMG}=10 ms, 16 averages, scan duration 5 minutes and 24 seconds.

The TRUST MRI data were processed using in-house Matlab scripts and standard image processing software. The images with the same effective TE were realigned using a 2D realignment script in SPM2 (University College London, UK). The images at different effective TEs and between scans were co-registered using FSL's function FLIRT (FMRIB Software Library, Oxford University, UK). The estimation of blood T2 from the TRUST data used procedures similar to those used previously (9,36). Briefly, after pair-wise subtraction between control and labeled images, a ROI was manually drawn to include the whole slice. The difference signals in the entire slice were averaged. Note that, although the signals in the control and labeled images have considerable partial voluming between vessel and tissue, the difference signals are expected to originate predominantly from vessels due to cancellation of static tissue signals. The averaged signals were fitted to a mono-exponential function to obtain T2. The 95% confidence interval of the estimation was also obtained.

The T2 values obtained from the TRUST data were compared to predicted T2 using PulsOx-measured Y_a and Centrifuge-measured Hct via the 3D calibration plot. Correlation analysis was performed between the predicted and experimental T2. As an alternative analysis, the TRUST-derived T2 and the Hct value was used to estimate the arterial oxygenation level during hypoxia and the results were compared to the PulsOx Y_a values.

Results

Calibration study

The data from the blood samples yielded highly reliable fitting. The 95% confidence intervals of the estimated 1/T2 were 0.31 s^{-1}, 0.32 s^{-1}, 0.48 s^{-1}, and 0.82 s^{-1} for τ_{CPMG} of 5 ms, 10 ms, 15 ms, and 20 ms, respectively. Slightly higher confidence interval was observed at τ_{CPMG} of 20 ms because the longer effective TE resulted in lower SNR in these data. Figure 1a shows a surface plot illustrating the relationship between blood T2, Y and Hct for the four τ_{CPMG} values. The symbols indicated the experimental data points and the mesh showed the model-fitted surface. The coefficients from the fitting are listed in Table 1. Figure 1b shows 2D sub-plots at fixed Hct and Y for varying τ_{CPMG}, demonstrating that longer τ_{CPMG} resulted in a smaller T2 but the overall feature of the curves is similar.

Validation study

Physiologic parameters during normoxia and hypoxia periods are summarized in Table 2. As expected, a significant decrease in arterial oxygen saturation fraction, Y_a, was observed when comparing hypoxia to normoxia ($P<0.001$). Et CO2 decreased by 3% ($P=0.008$) and heart rate increased by 13% ($P=0.002$). Breathing rate did not show a significant change between the two physiologic states ($P=0.55$). Figure 2 shows a representative TRUST dataset with control, labeled and difference images at four effective TEs. During normoxia, the blood T2 values were 154.2±13.1 ms (N=7, mean ± standard deviation). Since Y_a is close to unity during normoxia and is relative constant across subjects (Table 2), the variations in arterial T2 values are expected to be primarily attributed to Hct differences among individuals. Figure 3 shows a scatter plot between blood T2 and Hct, confirming a significant correlation between these parameters ($P=0.03$). This relationship may be potentially exploited for non-invasive estimation of Hct.

During the hypoxia period, the blood T2 measured with TRUST MRI was found to be 127.2±15.3 ms. Using the PulsOx-determined Y_a and Centrifuge-determined Hct, one can predict the blood T2 from the 3D calibration plot, which was found to be 128.6±18.4 ms. Figure 4 shows the scatter plot between the experimental and predicted T2 values for both physiologic conditions (red symbols: normoxia data, blue symbols: hypoxia data). A significant correlation was observed ($P<0.001$). In the alternative analysis, using TRUST T2 and Hct, we estimated the Y_a to be 0.837±0.036. These values are highly consistent with the gold-standard values measured with PulsOx (0.840±0.036). The differences between TRUST-derived and PulsOx-measured Y were 0.003±0.026.

Discussion

The present study establishes a comprehensive calibration plot that can be used to convert blood CPMG-T2 to oxygenation at 3 Tesla. Compared to previous studies, the present data account for Hct differences across individuals and have used a pulse sequence that matched the in vivo experiments (e.g. composite pulses, MLEV16 phase cycling), thus are expected to provide a more accurate estimation of Y. Although the calibration experiments were performed for the optimization of the TRUST technique, the plots can also be used for several other T2-based oxygen quantification methods (10,11,13,25,39). Furthermore, we validated the TRUST results in humans in a hypoxia setting. Hypoxia challenge by inhalation of 14% O2 was found to reduce the arterial oxygenation to approximately 0.84 according to the TRUST measurement and this was in excellent agreement with the gold-standard Pulse Oximetry values.

Techniques for quantitative estimation of blood oxygenation can be categorized into three main groups: susceptibility effect in extravascular tissue (14,15), phase angle in

intravascular blood signal (12,16), and T2 value of blood signal (9–11,13,25), with each method having certain advantages and disadvantages. The advantages of blood T2-based methods are that they do not require complex modeling and fitting of the data and that they are not sensitive to macroscopic field inhomogeneity or vessel orientation. A limitation of these methods is that the quantification requires a calibration plot that specifies the relationship between blood T2 and oxygenation. The calibration plot ideally should match the in vivo settings in terms of field strength, type of T2 (e.g. spin-echo T2 versus CPMG-T2), inter-echo spacings (τ_{CPMG}), RF pulse shape (e.g. block, sinc, or adiabatic), type (e.g. simple versus composite), phases, and Hct. Our previous TRUST MRI studies used a calibration plot that was obtained from equivalent field strength and τ_{CPMG} (9), but the details of the RF pulse were not matched. Therefore, by using identical TRUST sequences for in vitro and in vivo experiments, the present study can further improve the accuracy of this technique in oxygenation estimation. Moreover, the calibration data of this study extended the previous 2D plot to a 3D plot by also considering the effect of Hct on blood T2. All previous T2-based studies (9,11,13,25) have used a 2D calibration plot by assuming a typical Hct level. While this may be acceptable for group averaged data in which the biases due to Hct will cancel out across subjects, estimation of blood oxygenation on an individual basis requires the accounting of Hct effect. As an example, we have tested to use the 2D calibration plot (assuming Hct=0.4) in the validation data analysis, and the results showed that the correlation between the predicted and experimental T2 was less apparent (normoxia: R=0.47, P=0.29; hypoxia: R=0.82, P=0.025), compared to the 3D calibration results (normoxia: R=0.85, P=0.016; hypoxia: R=0.90, P=0.006).

The validation study demonstrated an excellent agreement between the TRUST-derived and PulsOx-measured Y_a values. The group-averaged values showed virtually no differences between these two measurement methods, although on the individual subject level the differences had a standard deviation of 0.026. This range is consistent with the measurement uncertainty of the arterial TRUST MRI used in this study, which was estimated to be 0.028 using a goodness-of-fit assessment (nlinfit.m in Matlab) in the T2 fitting. We note that, in venous TRUST studies which are the primary applications of this technique, we have previously estimated the fitting error to be 0.020 despite a shorter scan duration (9). This is because the venous oxygenation has a typical range of 0.5–0.75 (40) and within this range the slope between T2 and Y is greater (i.e. each unit of Y change causes a large T2 change, see Figure 1 for examples), rendering a higher sensitivity and accuracy for oxygenation estimation in the venous range.

This validation study took advantage of the ability of hypoxia in modulating arterial blood oxygenation, thus allowed us to use PulsOx as a gold-standard reference rather than using other modalities such as Positron Emission Tomography (PET) (2). PulsOx is routinely used in monitoring patient oxygenation levels in clinical settings and is considered of relatively high reliability (41). On the other hand, ^{15}O-based PET measurements are still a research tool and has lower sensitivity and accuracy even compared to MR measurements (42). We note that, although this study has primarily focused on the measurement and comparison of arterial oxygenation, the TRUST sequence has been successfully applied to the venous vessels as well (3,9,20–23), which is the main advantage of this new technique compared to current gold-standard methods such as PulsOx.

This study presented an empirical relationship between blood T2, Y, and Hct. In fitting the experimental data, we used a Luz-Meiboom two-site exchange model reported in a number of publications (10,13). There are alternative models based on water diffusion (28,29,43), and the data in the present study do not provide an assessment of the validity of either model or the theory underlying blood T2 relaxometry. The goal of this study is to establish a calibration plot for the conversion of blood T2 value to Y. The biophysical meaning of the

coefficients is limited. The experimental design for a blood relaxometry study would have been slightly different in that a larger range of Hct and Y would need to be sampled rather than the narrow but densely sampled physiologic range chosen in our study. Accordingly, the calibration plot established in this study should only be used for data within the physiological range.

The findings from the present study should be interpreted in view of a few limitations. The hypoxia challenge used in this study was only able to reduce the arterial oxygenation to a range of 0.79–0.89. While the MRI oxygenation estimation within this range was found to agree well with the gold-standard measures, the relevant range for venous blood (i.e. 0.5–0.75) was not tested. Although we expect the performance of the technique would be at least as good, if not better (due to a steeper slope as mentioned earlier), for the venous oxygenation, cautions should be used in extrapolation these data. In addition, the use of the 3D calibration plot requires the knowledge of the individual's Hct level, which may add extra burden to the participant. Of course one can still just assume a Hct value, or, alternatively use the arterial T2 value to estimate Hct, by including an additional scan of 5.5 minutes. Another potential approach is to use Hct values obtained in previous clinical tests, assuming the variations between the two time points are acceptable.

Conclusion

The present study provides an improved calibration plot for non-invasive estimation of blood oxygenation using TRUST MRI. The new plot employs imaging pulse sequences that better match the in vivo sequences and also accounts for the effects of Hct levels on relaxation rates. An in situ human validation study utilizing these calibration data further revealed that the TRUST-derived arterial blood oxygenation values were in excellent agreement with those measured with a PulsOx device. The availability of this new calibration curve is expected to enhance the use of TRUST MRI for the measurement of cerebral blood oxygenation and oxygen metabolism.

Acknowledgments

The authors would like to express gratitude to Dr. Jinsoo Uh for assistance with the pulse sequence programming. This publication was made possible in part by grant support from NIHNCRR P41-RR15241. The National Center for Research Resources (NCRR) is a component of the National Institutes of Health (NIH). The contents of the paper are solely the responsibility of the authors and do not necessarily represent the official view of NCRR or NIH. Equipment used in the study is manufactured by Philips. Dr. van Zijl is a paid lecturer for Philips Medical Systems. Dr. van Zijl is the inventor of technology that is licensed to Philips. This arrangement has been approved by Johns Hopkins University in accordance with its conflict of interest policies.

Grant Sponsors: NIH R01 MH084021, NIH R01 NS067015, NIH R01 AG033106, NIH-NCRR P41 RR015241

Appendix

Model describing the relationship between blood T2, Y and Hct

According to Equations [3–6] in Golay et al. (13), 1/T2 of blood (also known as R2) can be written as:

$$\frac{1}{T_2}=R_{2,0}+Hct\cdot(1-Hct)\cdot(\Delta\omega)^2\cdot\tau\left[1-\frac{2\tau}{\tau_{CPMG}}\tanh\left(\frac{\tau_{CPMG}}{2\tau}\right)\right] \quad [A1]$$

where

$$R_{2,0}=R_{2,plas}+Hct\cdot\left(R_{2,ery}-R_{2,plas}\right) \quad [A2]$$

and $R_{2,plas}$ and $R_{2,ery}$ are transverse relaxation rates of plasma and erythrocytes, respectively. $R_{2,ery}$ can in turn be written as:

$$R_{2,ery}=R_{2,plas}+R_{2,dia}+R_{2,oxy}+(1-Y)\left(R_{2,deoxy}-R_{2,oxy}\right) \quad [A3]$$

Applying Equation [A3] in [A2], one can write:

$$R_{2,0}=R_{2,plas}+Hct\cdot\left[R_{2,dia}+R_{2,oxy}+(1-Y)\left(R_{2,deoxy}-R_{2,oxy}\right)\right] \quad [A4]$$

The term Δω in Equation [A1] can be expanded as: Furthermore, the term $\tau\left[1-\frac{2\tau}{\tau_{CPMG}}\tanh\left(\frac{\tau_{CPMG}}{2\tau}\right)\right]$ in Equation [A1] is not dependent on Y or Hct, thus can be treated as a constant. We therefore define:

$$\Delta\omega=\omega_{dia}+\omega_{oxy}+(1-Y)\left(\omega_{deoxy}-\omega_{oxy}\right) \quad [A5]$$

Then, applying Equations [A4–6] in [A1], we have:

$$\mu=\tau\left[1-\frac{2\tau}{\tau_{CPMG}}\tanh\left(\frac{\tau_{CPMG}}{2\tau}\right)\right] \quad [A6]$$

Rearranging Equation [A7] in terms of (1−Y) and Hct, one can readily write:

$$\frac{1}{T_2}=R_{2,plas}+Hct\cdot\left[R_{2,dia}+R_{2,oxy}+(1-Y)\left(R_{2,deoxy}-R_{2,oxy}\right)\right]+Hct\cdot(1-Hct)\cdot\left[\omega_{dia}+\omega_{oxy}+(1-Y)\left(\omega_{deoxy}-\omega_{oxy}\right)\right]^2\cdot\mu \quad [A7]$$

where A, B and C are in turn dependent on Hct by:

$$\frac{1}{T_2}=A+B\cdot(1-Y)+C\cdot(1-Y)^2 \quad [A8]$$

$$A=R_{2,plas}+\left[R_{2,dia}+R_{2,oxy}+\mu\cdot\left(\omega_{dia}+\omega_{oxy}\right)^2\right]\cdot Hct-\mu\cdot\left(\omega_{dia}+\omega_{oxy}\right)\cdot Hct^2 \quad [A9]$$

$$B=\left[R_{2,deoxy}-R_{2,oxy}+2\mu\cdot\left(\omega_{dia}+\omega_{oxy}\right)\cdot\left(\omega_{deoxy}-\omega_{oxy}\right)\right]\cdot Hct-2\mu\cdot\left(\omega_{dia}+\omega_{oxy}\right)\cdot\left(\omega_{deoxy}-\omega_{oxy}\right)\cdot Hct^2 \quad [A10]$$

We can simplify the expressions by defining:

$$C=\mu\cdot\left(\omega_{deoxy}-\omega_{oxy}\right)^2\cdot Hct\cdot(1-Hct) \quad [A11]$$

$$a_1=R_{2,plas} \quad [A12]$$

$$a_2=R_{2,dia}+R_{2,oxy}+\mu\cdot\left(\omega_{dia}+\omega_{oxy}\right)^2 \quad [A13]$$

$$a_3=-\mu\cdot\left(\omega_{dia}+\omega_{oxy}\right)^2 \quad [A14]$$

$$b_1=R_{2,deoxy}-R_{2,oxy}+2\mu\cdot\left(\omega_{dia}+\omega_{oxy}\right)\cdot\left(\omega_{deoxy}-\omega_{oxy}\right) \quad [A15]$$

$$b_2=-2\mu\cdot\left(\omega_{dia}+\omega_{oxy}\right)\cdot\left(\omega_{deoxy}-\omega_{oxy}\right) \quad [A16]$$

and Equations [A9–11] can be rewritten into:

$$c_1=\mu\cdot\left(\omega_{deoxy}-\omega_{oxy}\right)^2 \quad [A17]$$

$$A=a_1+a_2\cdot Hct+a_3\cdot Hct^2 \quad [A18]$$

$$B=b_1\cdot Hct+b_2\cdot Hct^2 \quad [A19]$$

$$C=c_1\cdot Hct\cdot(1-Hct). \quad [A20]$$

These six coefficients, a_1, a_2, a_3, b_1, b_2, and c_1, are the outcomes of the model fitting.

References

1. Kety SS, Schmidt CF. The Effects of Altered Arterial Tensions of Carbon Dioxide and Oxygen on Cerebral Blood Flow and Cerebral Oxygen Consumption of Normal Young Men. J Clin Invest. 1948; 27:484–492.
2. Mintun MA, Raichle ME, Martin WR, Herscovitch P. Brain oxygen utilization measured with O-15 radiotracers and positron emission tomography. J Nucl Med. 1984; 25:177–187. [PubMed: 6610032]
3. Xu F, Ge Y, Lu H. Noninvasive quantification of whole-brain cerebral metabolic rate of oxygen (CMRO2) by MRI. Magn Reson Med. 2009; 62:141–148. [PubMed: 19353674]
4. Jain V, Langham MC, Wehrli FW. MRI estimation of global brain oxygen consumption rate. J Cereb Blood Flow Metab. 2010; 30:1598–1607. [PubMed: 20407465]
5. van Zijl PC, Eleff SM, Ulatowski JA, Oja JM, Ulug AM, Traystman RJ, Kauppinen RA. Quantitative assessment of blood flow, blood volume and blood oxygenation effects in functional magnetic resonance imaging. Nat Med. 1998; 4:159–167. [PubMed: 9461188]
6. Buxton RB, Frank LR, Wong EC, Siewert B, Warach S, Edelman RR. A general kinetic model for quantitative perfusion imaging with arterial spin labeling. Magn Reson Med. 1998; 40:383–396. [PubMed: 9727941]
7. Davis TL, Kwong KK, Weisskoff RM, Rosen BR. Calibrated functional MRI: mapping the dynamics of oxidative metabolism. Proc Natl Acad Sci U S A. 1998; 95:1834–1839. [PubMed: 9465103]
8. Hoge RD, Atkinson J, Gill B, Crelier GR, Marrett S, Pike GB. Linear coupling between cerebral blood flow and oxygen consumption in activated human cortex. Proc Natl Acad Sci U S A. 1999; 96:9403–9408. [PubMed: 10430955]
9. Lu H, Ge Y. Quantitative evaluation of oxygenation in venous vessels using T2-Relaxation-Under-Spin-Tagging MRI. Magn Reson Med. 2008; 60:357–363. [PubMed: 18666116]
10. Wright GA, Hu BS, Macovski A. Estimating oxygen saturation of blood in vivo with MR imaging at 1.5 T. J Magn Reson Imaging. 1991; 1:275–283. [PubMed: 1802140]
11. Oja JM, Gillen JS, Kauppinen RA, Kraut M, van Zijl PC. Determination of oxygen extraction ratios by magnetic resonance imaging. J Cereb Blood Flow Metab. 1999; 19:1289–1295. [PubMed: 10598932]
12. Haacke EM, Lai S, Reichenbach JR, Kuppusamy K, Hoogenraad FG, Takeichi H, Lin W. In vivo measurement of blood oxygen saturation using magnetic resonance imaging: a direct validation of the blood oxygen level dependent concept in functional brain imaging. Human Brain Mapping. 1997; 5:341–346. [PubMed: 20408238]
13. Golay X, Silvennoinen MJ, Zhou J, Clingman CS, Kauppinen RA, Pekar JJ, van Zijl PC. Measurement of tissue oxygen extraction ratios from venous blood T(2): increased precision and validation of principle. Magn Reson Med. 2001; 46:282–291. [PubMed: 11477631]
14. An H, Lin W. Impact of intravascular signal on quantitative measures of cerebral oxygen extraction and blood volume under normo- and hypercapnic conditions using an asymmetric spin echo approach. Magn Reson Med. 2003; 50:708–716. [PubMed: 14523956]
15. He X, Yablonskiy DA. Quantitative BOLD: mapping of human cerebral deoxygenated blood volume and oxygen extraction fraction: default state. Magn Reson Med. 2007; 57:115–126. [PubMed: 17191227]
16. Fernandez-Seara MA, Techawiboonwong A, Detre JA, Wehrli FW. MR susceptometry for measuring global brain oxygen extraction. Magn Reson Med. 2006; 55:967–973. [PubMed: 16598726]
17. St Lawrence KS, Wang J. Effects of the apparent transverse relaxation time on cerebral blood flow measurements obtained by arterial spin labeling. Magn Reson Med. 2005; 53:425–433. [PubMed: 15678532]
18. Wells JA, Lythgoe MF, Choy M, Gadian DG, Ordidge RJ, Thomas DL. Characterizing the origin of the arterial spin labelling signal in MRI using a multiecho acquisition approach. J Cereb Blood Flow Metab. 2009; 29:1836–1845. [PubMed: 19654586]

19. Lu H, Zhao C, Ge Y, Lewis-Amezcua K. Baseline blood oxygenation modulates response amplitude: Physiologic basis for intersubject variations in functional MRI signals. Magn Reson Med. 2008; 60:364–372. [PubMed: 18666103]
20. Lu H, Yezhuvath US, Xiao G. Improving fMRI sensitivity by normalization of basal physiologic state. Hum Brain Mapp. 2010; 31:80–87. [PubMed: 19585589]
21. Lu H, Xu F, Rodrigue KM, Kennedy KM, Cheng Y, Flicker B, Hebrank AC, Uh J, Park DC. Alterations in Cerebral Metabolic Rate and Blood Supply across the Adult Lifespan. Cereb Cortex. 2010 doi: 10.1093/cercor/bhq1224; In-press.
22. Ge, Y.; Zhang, Z.; Lu, H.; Tang, L.; Jaggi, H.; Herbert, J.; Babb, JS.; Grossman, RI. Proc Intl Soc Mag Reson Med. Montreal, Canada: 2011. Characterizing Brain Oxygen Metabolism in Patients with Multiple Sclerosis with T2-Relaxation-Under-Spin-Tagging (TRUST) MRI.
23. Xu F, Uh J, Brier MR, Hart J Jr. Yezhuvath US, Gu H, Yang Y, Lu H. The influence of carbon dioxide on brain activity and metabolism in conscious humans. J Cereb Blood Flow Metab. 2011; 31:58–67. [PubMed: 20842164]
24. Xu, F.; Yezhuvath, US.; Liu, P.; Lu, H. Proc Intl Soc Mag Reson Med. Stockholm, Sweden: 2010. Hypoxia and hyperoxia alter brain metabolism in awake human; p. 1032
25. Qin Q, Grgac K, van Zijl PC. Determination of whole-brain oxygen extraction fractions by fast measurement of blood T(2) in the jugular vein. Magn Reson Med. 2011; 65:471–479. [PubMed: 21264936]
26. Silvennoinen MJ, Clingman CS, Golay X, Kauppinen RA, van Zijl PC. Comparison of the dependence of blood R2 and R2* on oxygen saturation at 1.5 and 4.7 Tesla. Magn Reson Med. 2003; 49:47–60. [PubMed: 12509819]
27. Zhao JM, Clingman CS, Narvainen MJ, Kauppinen RA, van Zijl PC. Oxygenation and hematocrit dependence of transverse relaxation rates of blood at 3T. Magn Reson Med. 2007; 58:592–597. [PubMed: 17763354]
28. Chen JJ, Pike GB. Human whole blood T2 relaxometry at 3 Tesla. Magn Reson Med. 2009; 61:249–254. [PubMed: 19165880]
29. Stefanovic B, Pike GB. Human whole-blood relaxometry at 1.5 T: Assessment of diffusion and exchange models. Magn Reson Med. 2004; 52:716–723. [PubMed: 15389952]
30. Lu H, Clingman C, Golay X, van Zijl PC. Determining the longitudinal relaxation time (T1) of blood at 3.0 Tesla. Magn Reson Med. 2004; 52:679–682. [PubMed: 15334591]
31. Benga G, Borza T. Diffusional water permeability of mammalian red blood cells. Comp Biochem Physiol B Biochem Mol Biol. 1995; 112:653–659. [PubMed: 8590380]
32. Yezhuvath US, Lewis-Amezcua K, Varghese R, Xiao G, Lu H. On the assessment of cerebrovascular reactivity using hypercapnia BOLD MRI. NMR Biomed. 2009; 22:779–786. [PubMed: 19388006]
33. Wong EC. Vessel-encoded arterial spin-labeling using pseudocontinuous tagging. Magn Reson Med. 2007; 58:1086–1091. [PubMed: 17969084]
34. Wu WC, Fernandez-Seara M, Detre JA, Wehrli FW, Wang J. A theoretical and experimental investigation of the tagging efficiency of pseudocontinuous arterial spin labeling. Magn Reson Med. 2007; 58:1020–1027. [PubMed: 17969096]
35. Gonzalez-At JB, Alsop DC, Detre JA. Cerebral perfusion and arterial transit time changes during task activation determined with continuous arterial spin labeling. Magn Reson Med. 2000; 43:739–746. [PubMed: 10800040]
36. Liu P, Uh J, Lu H. Determination of spin compartment in arterial spin labeling MRI. Magn Reson Med. 2011; 65:120–127. [PubMed: 20740655]
37. Kuhl DE, Alavi A, Hoffman EJ, Phelps ME, Zimmerman RA, Obrist WD, Bruce DA, Greenberg JH, Uzzell B. Local cerebral blood volume in head-injured patients. Determination by emission computed tomography of 99mTc-labeled red cells. J Neurosurg. 1980; 52:309–320. [PubMed: 7359185]
38. Aslan S, Xu F, Wang PL, Uh J, Yezhuvath US, van Osch M, Lu H. Estimation of labeling efficiency in pseudocontinuous arterial spin labeling. Magn Reson Med. 2010; 63:765–771. [PubMed: 20187183]

39. Bolar, DS.; Rosen, BR.; Sorensen, AG.; Adalsteinsson, E. Proc Intl Soc Mag Reson Med. Honolulu, HI: 2009. Quantitative Imaging of extraction of oxygen and tissue consumption using velocity selective spin labeling; p. 628

40. Coles JP, Minhas PS, Fryer TD, Smielewski P, Aigbirihio F, Donovan T, Downey SP, Williams G, Chatfield D, Matthews JC, Gupta AK, Carpenter TA, Clark JC, Pickard JD, Menon DK. Effect of hyperventilation on cerebral blood flow in traumatic head injury: clinical relevance and monitoring correlates. Crit Care Med. 2002; 30:1950–1959. [PubMed: 12352026]

41. Van de Louw A, Cracco C, Cerf C, Harf A, Duvaldestin P, Lemaire F, Brochard L. Accuracy of pulse oximetry in the intensive care unit. Intensive Care Med. 2001; 27:1606–1613. [PubMed: 11685301]

42. Uh J, Lin AL, Lee K, Liu P, Fox P, Lu H. Validation of VASO cerebral blood volume measurement with positron emission tomography. Magn Reson Med. 2011; 65:744–749. [PubMed: 21337407]

43. Jensen JH, Chandra R. NMR relaxation in tissues with weak magnetic inhomogeneities. Magn Reson Med. 2000; 44:144–156. [PubMed: 10893533]

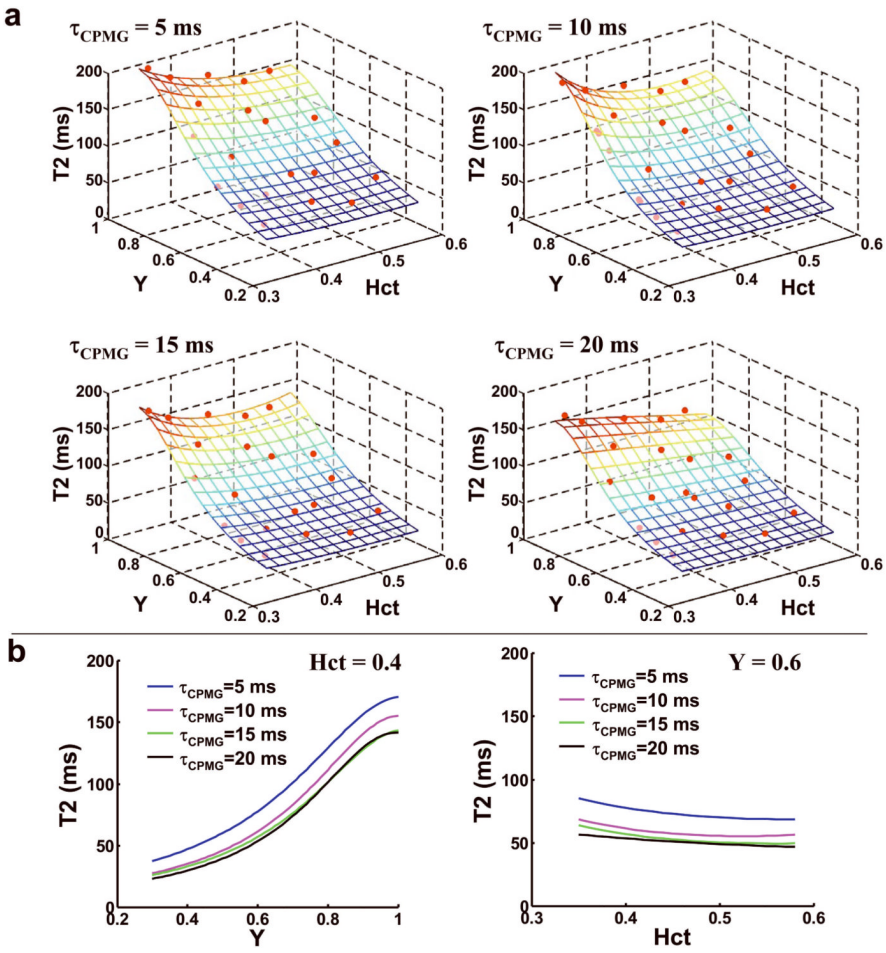

Figure 1.

Relationship between T2, Y, and Hct in blood samples. (a) T2 values of blood samples as a function of oxygenation (Y) and hematocrit (Hct) at four different τ_{CPMG}. The symbols indicated the experimental data points and the mesh showed the model-fitted surface. The surface was displayed with partial transparency thus the symbols below the surface can also be seen, although with a slightly darker color. The values of Y and Hct were written in fractions. The analytical expressions of the surfaces are listed in Equations [1–4] and Table 1. (b) Two-dimensional plots between T2 and Y at a fixed Hct of 0.4 and between T2 and Hct at a fixed Y of 0.6. Each plot shows curves at four different τ_{CPMG} values.

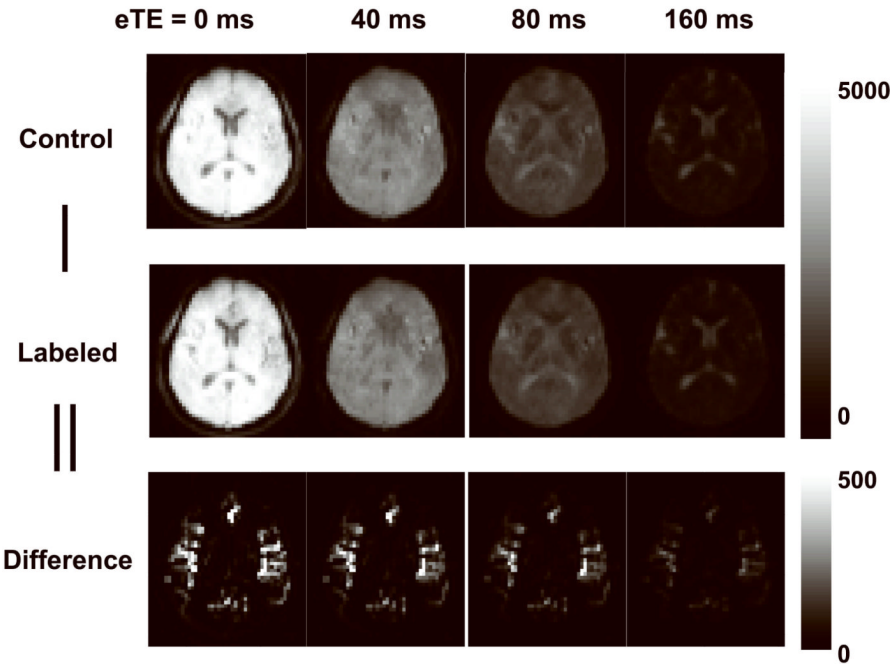

Figure 2.

Representative images from TRUST MRI. The scan acquired control and labeled images in an interleaved fashion. Each image type was acquired at four different T2-weightings as indicated by the effective TE (eTE). The difference images were calculated from the subtractions. The difference images are displayed in a different color scale because their signal intensities are considerably lower than the control and labeled images.

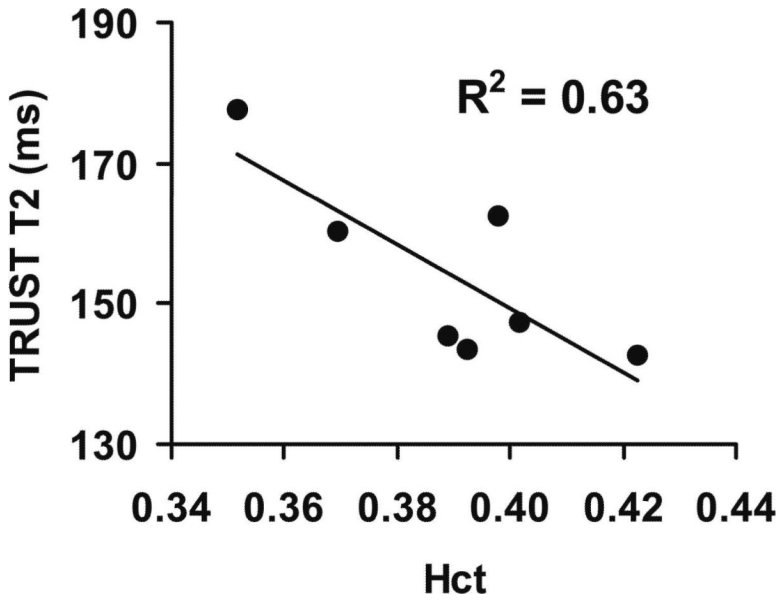

Figure 3.

Relationship between arterial blood T2 and hematocrit in humans during normoxia. The T2 was measured using TRUST MRI and the Hct was determined with a centrifuge. The arterial blood was close to full oxygenation under this condition (Y_a=0.973±0.006). The T2 was therefore primarily dependent upon the Hct levels. The solid line represents the linear fitting curve. This plot is based entirely on the in vivo data, and did not involve the calibration data.

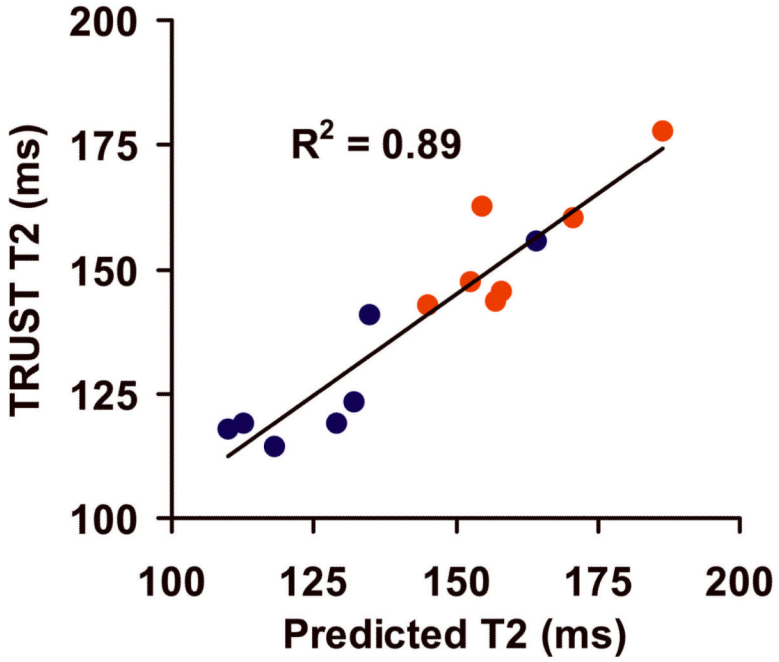

Figure 4.
Scatter plot between TRUST-determined blood T2 values and those predicted using the calibration plot with individual Y_a and Hct. Red symbols indicate normoxia data points. Blue symbols indicated hypoxia data points. The solid line represents the linear fitting curve.

Table 1

Fitted coefficients for the model described in Equations [1–4]. These coefficients completely characterize the relationship between blood T2, Y and Hct at a specific τ_{CPMG}.

	a_1 (s^{-1})	a_2 (s^{-1})	a_3 (s^{-1})	b_1 (s^{-1})	b_2 (s^{-1})	c_1 (s^{-1})
τ_{CPMG} = 5 ms	−4.4	39.1	−33.5	1.5	4.7	167.8
τ_{CPMG} = 10 ms	−13.5	80.2	−75.9	−0.5	3.4	247.4
τ_{CPMG} = 15 ms	−12.0	77.7	−75.5	−6.6	31.4	249.4
τ_{CPMG} = 20 ms	7.0	−9.2	23.2	−4.5	5.3	310.8

Table 2

Physiologic parameters during normoxia and hypoxia.

	Y_a (in fraction)	Et CO2 (mmHg)	Heart rate (bpm)	Breathing rate (bpm)
Normoxia	0.973±0.006	43.4±2.7	68.2±13.4	15.6±2.6
Hypoxia	0.840±0.036	42.1±2.2	77.1±14.7	15.8±3.8